

# Top quark phenomenology of the ADD model and the Minimal Length Scenario

K. Mimasu and S. Moretti

*School of Physics & Astronomy,  
University of Southampton, Southampton, SO17 1BJ, UK*

## Abstract

We study top-(anti)quark pair production at the Tevatron and Large Hadron Collider (LHC) in the context of the Minimal Length Scenario (MLS) of the Arkani-Hamed, Dimopoulos and Dvali (ADD) model of extra dimensions (XDs). We show that sizable effects onto both the integrated and differential cross section due to graviton mediation are expected for a String scale,  $M_S$ , of  $\mathcal{O}(1-10 \text{ TeV})$  and several XDs,  $\delta$ , all compatible with current experimental constraints. Potential limits on  $M_S$  are extracted. We also highlight clear phenomenological differences between a simple ADD scenario and its modification based on using the MLS as a natural regulator for divergent amplitudes of virtual KK graviton exchange.

## 1 Introduction

Models of extra dimensions (XDs) have emerged in the past decade or so as an alternative approach to physics Beyond the Standard Model (BSM). Although such notions were conceived almost a century ago, it took until the advent of String theory to place them on a sound theoretical footing, culminating in the proposal by Arkani-Hamed, Dimopoulos and Dvali [1] of large XDs. Known as the ADD model, it reformulated the gauge hierarchy problem of the Standard Model (SM) in terms of compact extra dimensions in which only gravity can propagate. This dilutes the strength of gravity relative to other forces and reconciles the observed Planck mass,  $M_P$ , with the Electro-Weak (EW) scale via a new fundamental string scale,  $M_S$ , associated with gravity in the bulk. The relatively large volume of such XDs can lower the effective gravity scale to  $\mathcal{O}(\text{TeV})$ , which leads to the phenomenologically interesting case where gravitational effects could be observed at modern collider experiments. The

relationship between the two scales (Planck and String) in terms of the volume of  $\delta$  extra spatial dimensions goes as

$$M_P^2 = V_\delta M_S^{2+\delta}. \quad (1)$$

All SM degrees of freedom are confined to a 3-brane embedded in the bulk, a scenario that can be realised in String theory [2]. Such models can be understood as low energy effective realisations of String type theories where bulk gravitons emerge in 4 dimensions as infinite towers of Kaluza-Klein (KK) modes coupling to the SM with a strength suppressed by  $M_P$ . Accounting for the sum over all of these modes, however, leads to an effective coupling of order  $1/M_S$ . Therefore, one could observe effects due to real and virtual production of KK gravitons at the Tevatron and the Large Hadron Collider (LHC) through exotic missing energy signals and anomalous angular distributions as well as statistically significant deviations from those SM cross sections which are known precisely.

Another concept that arises from String theory is that of a minimum length scale below which one cannot probe. In short, if the energy of a String reaches  $M_S$ , perturbative String theory tells us that excitations would cause its extension [3]. The aforementioned possibility that the String scale can be lowered to experimentally accessible energies allows for a minimal length,  $l_S (\sim 1/M_S)$ , to also have phenomenological consequences. In particular, it can provide a mechanism to smoothly regularise Ultra-Violet (UV) divergences that occur in the amplitudes for virtual KK graviton production [4].

We describe a study of the ADD model extended with this phenomenological interpretation of a Minimum Length Scenario (MLS) in the context of virtual graviton exchange in the  $t\bar{t}$  channel at current hadron collider experiments. The aim is to determine the reach of the Tevatron and the LHC to set bounds on  $M_S$  by considering effects on the total  $pp(\bar{p}) \rightarrow t\bar{t}$  production cross section as well as various differential distributions due to the ADD model and its MLS extension. This is inspired by a similar study conducted on the Drell-Yan (DY) channel in [5]. While the di-lepton channel is the most common probe of the ADD model, other studies considering  $t\bar{t}$  in the context of the ADD model have also focused on the spin properties of KK gravitons to extract spin correlations [6]. As will be discussed later, the  $t\bar{t}$  channel becomes important at the LHC due to the dominance of gluon initial states, especially in the context of the ADD model where interference terms with the SM in the  $gg$  channel are the main contribution to observable deviations.

This paper is organised as follows. Sec. 2 goes into some more details of the ADD model and the consequences of its MLS extension. In Sec. 3, we consider the model in terms of  $t\bar{t}$  production at hadron colliders. Sec. 4 presents our results. Finally, we summarise and conclude in Sec. 5.

## 2 Large XDs and the MLS

### 2.1 The ADD model

The ADD model represents a simple realisation of  $\delta$  transverse extra dimensions, where the SM is fixed to exist on a 3-brane embedded in the bulk and the fundamental scale,  $M_S$ , is low ( $\mathcal{O}(\text{TeV})$ ). The bulk has the structure of a product space of 4-dimensional (4D) Minkowski space and a  $\delta$  dimensional compact subspace, chosen to be a torus with a common compactification radius,  $R$ , for simplicity ( $M_4 \times T_\delta$ ). This amounts to a model of linearised gravity in  $D = 4 + \delta$  dimensions where the degrees of freedom arise from fluctuations of the induced metric on the brane about flatness. The  $D$  dimensional graviton breaks down into a 4D graviton,  $\delta$  vectors and  $\delta(\delta + 1)/2$  scalars – corresponding to the zero modes of the KK spectrum. Above these lie infinite towers of closely spaced KK modes with masses  $m_n = 2\pi|\vec{n}|/R$ , where  $\vec{n} = (n_1, n_2, \dots, n_\delta)$ , with  $n_i$  labelling the KK number in each extra dimensional direction. After fixing the residual gauge freedom from general coordinate transformations one is left with a massive graviton,  $\delta - 1$  vectors and  $\delta(\delta - 1)/2$  scalars [7] per KK level.

This study follows the definitions and conventions established in [8] where KK decomposition shows that the vector and all but one scalar decouple from the SM while the gravitons,  $h_{\mu\nu}^{\vec{n}}$ , couple universally to the energy-momentum tensor. The remaining scalar degree of freedom,  $\phi^{\vec{n}}$ , couples to the trace of the energy-momentum tensor. This is the ‘radion’ associated with fluctuations of the size of the XDs. The effective interaction Lagrangian in 4D can be shown to be [8]:

$$\mathcal{L}_{int} = -\frac{\kappa}{2}(h_{\mu\nu}^{\vec{n}}T^{\mu\nu} + \phi^{\vec{n}}T_{\mu}^{\mu}), \quad \text{where} \quad T_{\mu\nu} \equiv -\eta_{\mu\nu}\mathcal{L}_{SM} + 2\frac{\delta\mathcal{L}_{SM}}{\delta g^{\mu\nu}}\Big|_{g_{\mu\nu}=\eta_{\mu\nu}} \quad (2)$$

and the coupling constant is defined as  $\kappa^2 = 16\pi/M_P^2$ .

The fact that the SM is localised on the brane means that, in the limit of a weak gravitational field, one can consider the energy-momentum tensor to have KK modes independent of  $n$ , which provides the universal coupling of all graviton excitations in energy regimes lower than the cutoff  $M_S$ , as discussed in [9]. The effects due to bulk deformations of the SM brane are not considered here in that its tension is assumed to be very large ( $\gg M_S$ ) and hence the ‘branons’ very heavy.

### 2.2 Virtual gravitons and the MLS

The Feynman rules for the vertices coupling the graviton to the SM are summarised in [8]; from these, one can calculate Matrix Elements (MEs) and hence cross sections for processes such as the one of interest:  $pp(\bar{p}) \rightarrow t\bar{t}$ . In the SM this is dominated by Quantum Chromodynamics (QCD) with a tiny EW contribution while in the ADD model it is mediated by an  $s$ -channel virtual KK graviton. Since the initial state particles can be assumed to be massless, the contribution from the scalar graviton sector is negligible due to its coupling to

the trace of  $T_{\mu\nu}$ . What remains is to sum up the contributions from all KK modes. This is dealt with in the appendix of [8] by treating the sum over many propagators as an integral over the KK mode mass:

$$D(p^2) = \sum_{\vec{n}} \frac{1}{p^2 - m_n^2 + i\epsilon} \Rightarrow \int^{\Lambda^2} \frac{\rho(m_n) dm_n^2}{p^2 - m_n^2 + i\epsilon}, \quad (3)$$

where the tensor structure of the numerator has been dropped. The density function,  $\rho(m_n)$ , accounts for degenerate KK levels. The tree-level amplitude for the mediation of a virtual KK graviton gains an effective coupling factor,  $\lambda_{\text{eff}}$ , from this integral:

$$\lambda_{\text{eff}} \sim D(s) \kappa^2 \sim \frac{F(\hat{s}, \delta)}{M_S^4} P \left[ I \left( \frac{M_S}{\sqrt{\hat{s}}} \right) \right]; \quad I \left( \frac{M_S}{\sqrt{\hat{s}}} \right) = \int_0^{M_S/\sqrt{\hat{s}}} dy \frac{y^{\delta-1}}{1-y^2}, \quad (4)$$

where  $F$  is a function of the partonic centre of mass (CM) energy,  $\hat{s}$ , and the number of XDs while  $P$  denotes the principal part of the integral. A hard cutoff associated with  $M_S$  must be introduced due to the divergent nature of this integral.

The MLS – defined as the incorporation of a minimum length,  $l_S$ , into the ADD setup – provides an alternative mechanism for regularising these divergences. If one assumes this scenario the uncertainty in position measurement can no longer be less than  $l_S$ . This entails a modification of the relationship between momentum  $p$  and wave vector  $k$  such that, whilst particle momentum can become arbitrarily high, the wave vector is bounded by  $1/l_S$ . A simple parametrisation that captures the essence of a MLS is that of the Unruh relations [10]:

$$\begin{aligned} k(p) &= \frac{1}{l_S} \tanh^{1/\gamma} \left[ \left( \frac{p}{M_S} \right)^\gamma \right], \\ \omega(E) &= \frac{1}{l_S} \tanh^{1/\gamma} \left[ \left( \frac{E}{M_S} \right)^\gamma \right], \end{aligned} \quad (5)$$

where  $\gamma$  is henceforth assumed to be 1 for simplicity<sup>1</sup>. As discussed in [4], this scenario brings about a number of modifications to the calculations. Most importantly, the new relations modulate the KK mode mass integral by a factor  $\partial\omega/\partial E$  to smoothly cut off the integral, which now becomes [5]

$$I' = \int_0^\infty dy \frac{y^{\delta-1}}{1-y^2} \text{sech}^2 \left( \frac{\sqrt{\hat{s}}}{M_S} y \right). \quad (6)$$

The integral is finite and can be evaluated numerically. Thus the requirement of a minimal length removes the need for a hard energy cutoff.

Another important modification due to this assumption affects the phase space measure, which is shown in [4] to lead to a change in the expression for the fully differential cross

---

<sup>1</sup>Different choices of  $\gamma$  simply would correspond to alternative ways of reaching  $1/l_S$ , while the asymptotic behaviour would remain the same. The limit  $\gamma \rightarrow \infty$  tends toward recovering a hard cutoff at  $M_S$ .

section:

$$d\tilde{\sigma} = d\sigma \prod_n \frac{E_n}{\omega_n} \prod_\nu \frac{\partial k_\nu}{\partial p_\nu}. \quad (7)$$

It is important to stress the phenomenological interpretation of the MLS that is applied in this study. We consider it as a useful mechanism for regulating the KK mass integrals rather than a concrete statement on the geometry of spacetime or the physics beyond  $M_S$ . For example, an issue that lies beyond the scope of this work is that of Lorentz symmetry violation, briefly discussed in [4], coming from the non-linear relationship between  $p$  and  $k$ . The MLS is treated here as a mechanism for regularising integrals whereas various other works elaborate in a more rigorous way upon notions of corrections to the uncertainty relations as well as of modifications to the Lorentz group action in the context of a minimum length or maximum momentum scale [11].

### 3 The $pp(\bar{p}) \rightarrow t\bar{t}$ process in the ADD model

A typical cross section for a SM process including ADD effects will take the form:

$$\sigma_{\text{tot}} = \sigma_{\text{SM}} + \sigma_{\text{int}}[\mathcal{O}(\lambda_{\text{eff}})] + \sigma_{\text{ADD}}[\mathcal{O}(\lambda_{\text{eff}}^2)], \quad (8)$$

where  $\sigma_{\text{int}}$  and  $\sigma_{\text{ADD}}$  denote the interference and pure ADD contributions, respectively and  $\lambda_{\text{eff}}$  is defined as in eqn. 4. For the QCD dominated  $t\bar{t}$  production, the  $q\bar{q}$  initial state is mediated by a gluon, meaning that the colour structure of the QCD diagram prevents interference with the ADD one. Through the  $gg$  initial state, in contrast, the SM diagram can interfere with the ADD one in the  $t$  and  $u$ -channels as shown in figure 1.

$$|\mathcal{M}_{\text{int}}|^2 = \left( \sum_{\vec{n}} \text{Diagram 1} \right) \times \left( \text{Diagram 2} + \text{Diagram 3} \right)$$

Diagram 1: A gluon exchange between two quark lines, labeled  $G_{\mu\nu}^{\vec{n}}$ .  
Diagram 2: A gluon exchange in the  $t$ -channel between two quark lines.  
Diagram 3: A gluon exchange in the  $u$ -channel between two quark lines.

Figure 1: Feynman diagrams showing schematically the interference between tree-level contributions to  $gg \rightarrow t\bar{t}$  of ADD and QCD.

One would therefore expect the LHC to be a particularly suitable environment to probe the ADD model and set bounds on its parameters, indeed more than the (mostly  $q\bar{q}$  mediated) Tevatron. This lends weight to the use of the  $t\bar{t}$  channel as a worthwhile addition to the various other analyses aiming to constrain large extra dimensions. The amplitudes for the processes  $gg \rightarrow t\bar{t}$  and  $q\bar{q} \rightarrow t\bar{t}$  have been published in [16], including both the interference and pure ADD terms. The squared amplitudes due to pure QCD were taken from MadGraph [17]. EW processes were also taken into account, but merely for completeness, as their effect was practically negligible.

Based on these results, we used Monte Carlo methods to generate invariant mass distributions and total cross sections for the ADD model with and without the MLS over a region of  $(M_S, \delta)$  parameter space at three benchmark collider setups: LHC at 14 TeV, Tevatron and ‘early data’ LHC at 7 TeV. In each case we assumed an integrated luminosity of 100, 5 and 4 fb<sup>-1</sup>, respectively. By comparing these data to SM predictions, the aim is to make statements about the reach of the experiments and their capacity to extract XD effects or else set bounds on the corresponding parameters. Most results presented here exploited the invariant mass of the final state,  $M_{tt}$ . In addition, comparisons in the so called ‘centrality ratio’,  $\chi = \exp(|y_1 - y_2|)$ , were also considered, where  $y_{1,2}$  are the rapidities of the two final state top (anti)quarks. A recent study on early LHC data [18] used an effective operator approach to ADD type models to extract powerful bounds on the effective coupling of the main operators that contribute to the dijet cross section using this variable. This prompted us to include  $\chi$  in our study. The translation of the bounds obtained from this paper to bounds on the fundamental scale of a specific model of large XD’s depends on how the KK graviton sum is regulated. The reach obtained in this study extends beyond current experimental constraints and we argue in the next section that a smooth cutoff prescription along with the phase space corrections brought about by the MLS lessen the risk of overestimating ADD contributions at energies near the cutoff scale in lieu of a full understanding of the high energy theory.

## 4 Results

A numerical routine was used to calculate the total cross sections integrated over a range of invariant mass,  $M_{tt}$ , for a choice of values of  $M_S$  in both the ADD and ADD-MLS models and compared to the SM, taking into account both the gluon and quark initial states. The corrections to the effective coupling and the phase space coming from the MLS were implemented with the guidance of [4], as described in section 2. The CTEQ6 Parton Distribution Functions (PDFs) [19] were used to compute the hadronic cross sections, with  $Q^2 = (2m_t)^2$ . No higher order effects were considered, neither in the SM nor for the ADD model in order to consistently compare tree level predictions. This is done with the confidence that the cross section is well known to Next-to-Leading Order (NLO) accuracy in the full SM [20] and therefore normalisation to the SM background is not an issue, rather we focus on the potential to observe deviations from predictions due to the ADD and the MLS dynamics. All data shown (except in subsecs. 4.2 and 4.3) correspond to the LHC at 14 TeV as, in general, the other benchmark collider setups neither show qualitatively different results nor offer better sensitivity.

### 4.1 Differential cross sections

#### 4.1.1 Invariant mass

We start our analysis by looking at the differential cross section in invariant mass of the top-antitop pair,  $M_{tt}$ , for the purpose of determining the ranges over which to integrate

upon in order to extract good signal-to-background ratios. This also provides information about energy regimes in which the validity of such effective theories may be called into question. Unlike the total cross section, invariant mass distributions give some insight into the behaviour near the cutoff,  $M_S$ , where one would expect the effective model to start breaking down. This is reflected in Fig. 2 where the ADD cross section appears in fact to diverge near  $M_S$  and where we can also highlight the naturally regulating feature of its MLS extension, which does not have this asymptotic behaviour.

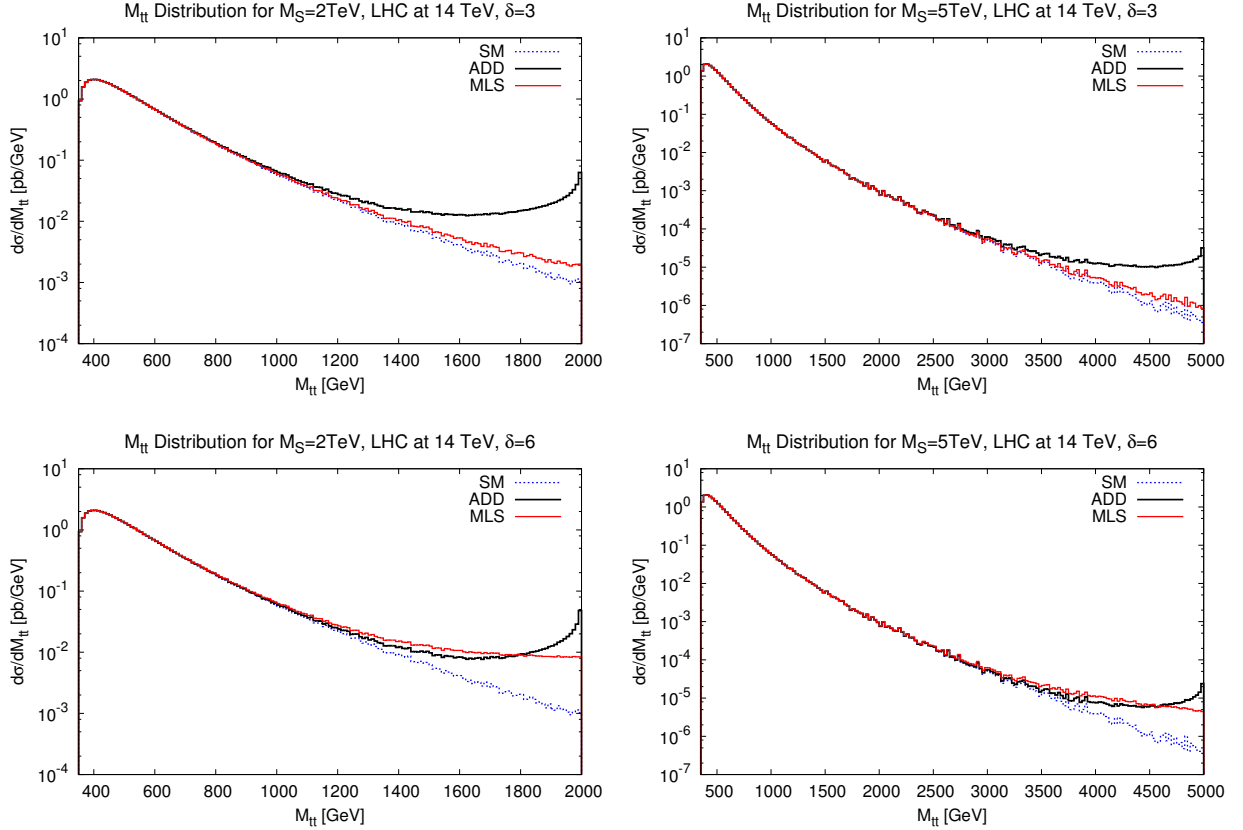


Figure 2: Differential cross sections w.r.t. the  $t\bar{t}$  invariant mass,  $M_{t\bar{t}}$ , at the LHC at 14 TeV for  $M_S = 2$  and 5 for the SM, ADD and ADD-MLS for  $\delta = 3(6)$  XDs [*upper(lower)*].

The absence of such divergence in the MLS case shows that the  $\sim \text{sech}^2(\frac{\sqrt{s}}{M_S})$  suppression in the mass integral works in taming the effective coupling while the phase space factors also further deplete the cross section at high invariant mass. This leads to the conclusion that a valid comparison of all models can occur only if one does not integrate up to  $M_S$  but up to somewhere like  $0.8M_S$ , where one starts to see an unnatural enhancement of the ADD cross section, thus avoiding an over-estimation of the ADD contribution. We find that it may be difficult to produce any observable deviation from the SM at very high  $M_S$ , especially when it is above the collider energy.

The figures also provide guidance on the minimum invariant mass cuts needed for the eventual total cross section calculations. A ‘tracking’ invariant mass cut of  $M_{t\bar{t}} > M_S/2$  was decided upon as a simple and effective one to implement. It is interesting to note that, over most of the range where deviation from the SM differential cross section occurs, the MLS spectrum becomes more and more comparable to the ADD one as the number of XDs is increased, surpassing it at  $\delta = 6$ . This is a consequence of the fact that the MLS allows one to integrate over the whole range of KK modes while the ADD restricts the process to the exchange of modes up to the effective cutoff,  $M_S$  (compare eqns. 4 and 6). Fig. 3 highlights the behaviour of the two models with varying  $\delta$ .

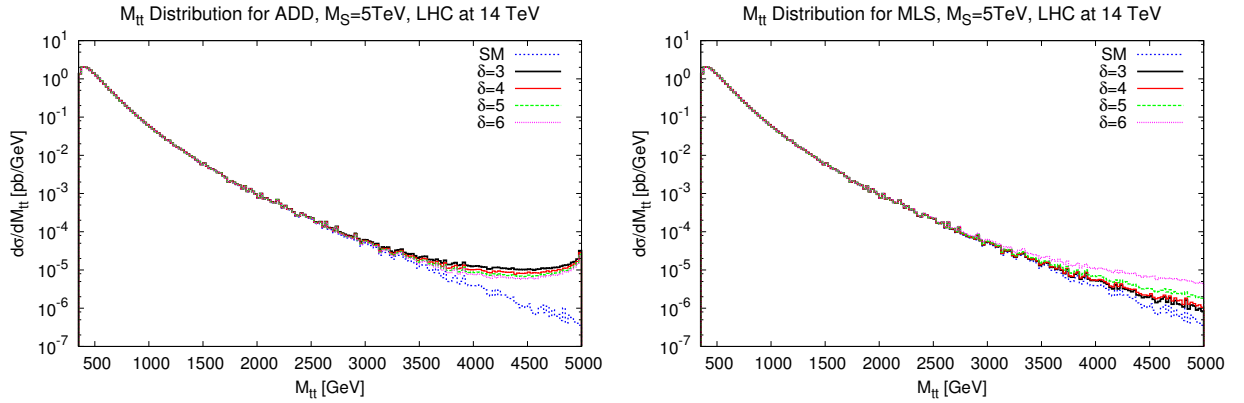


Figure 3: Variation with the number of XDs,  $\delta$ , of the differential cross sections w.r.t. the  $t\bar{t}$  invariant mass,  $M_{t\bar{t}}$ , for the LHC at 14 TeV and  $M_S = 5$  TeV shown in the ADD and ADD-MLS scenarios.

#### 4.1.2 Centrality ratio

Another useful differential observable is the centrality ratio,  $\chi$ , defined as  $\exp(|y_1 - y_2|) \equiv \exp(|2y^*|)$ , where  $y_{1,2}$  are the rapidities of the final state particles in the collider frame and  $y^*$  is the rapidity in the CM frame. In eliminating the boost of the collider frame, it allows for a better comparison of angular distributions. The ADD and MLS processes proceed via the exchange of a spin-2 graviton which involves terms with a different ( $\sim \cos^4 \theta$ ) angular dependence to the SM background, making  $\chi$  an effective and robust discriminating variable.

Fig. 4 shows the distributions normalised to 1 for  $\delta = 3, 6$  XDs, implementing the tracking invariant mass cuts discussed in section 4.1.1. Clearly,  $\chi$  is a powerful variable at the LHC (at both energies) as the ADD and MLS contribute significantly more in the low region (while this is not so at the Tevatron). The shoulders appearing in some of the distributions are an artefact of the invariant mass cuts and correspond to the  $\chi$  value at the minimum invariant mass as  $\cos \theta$  in the CM frame tends to 1. Additional cuts of  $\chi < 4$  optimised to improve



LHC reach were decided upon based on these. Although not addressed any further in this study, this variable may indeed be one of the best choices for directly setting bounds on signals induced by virtual gravitons, as applied in [18]. However, obtaining accurate angular information based on reconstructed  $t\bar{t}$  final states is non-trivial.

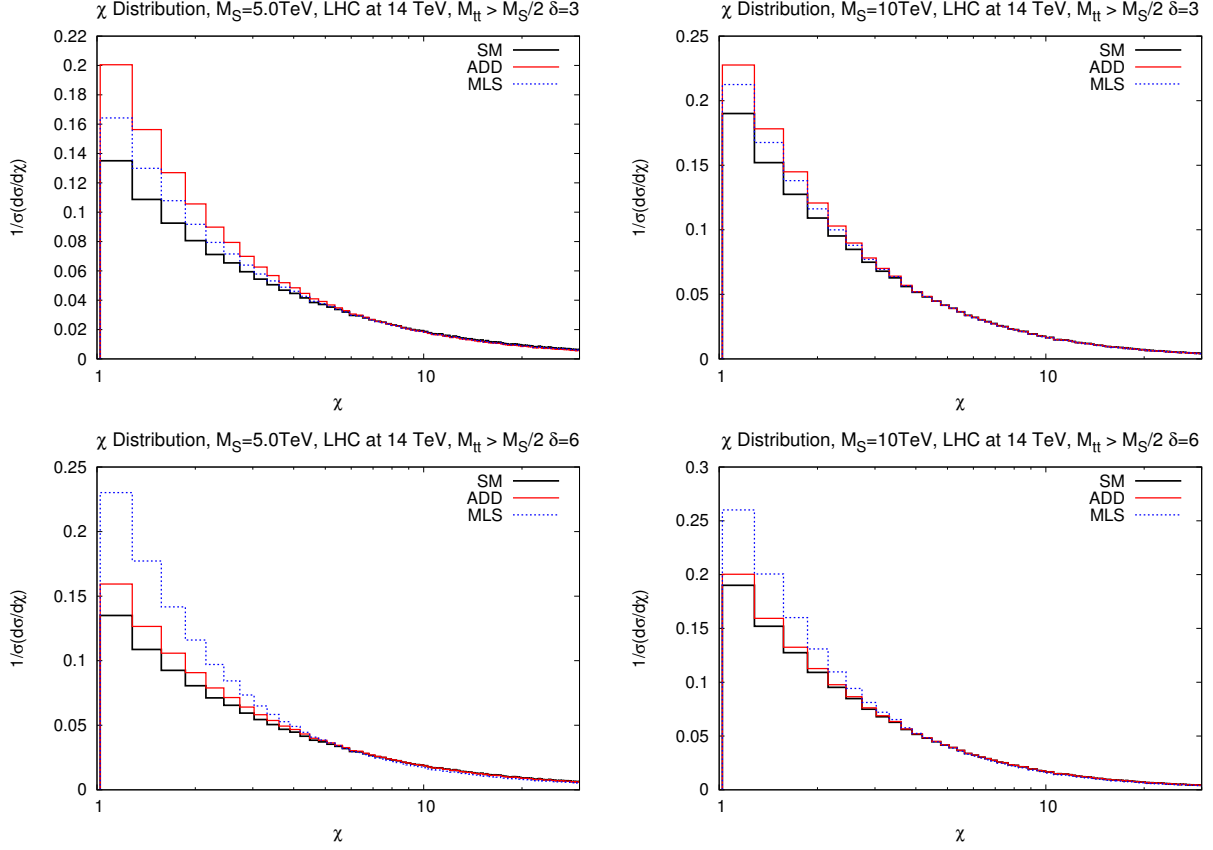


Figure 4: Differential cross sections w.r.t. the centrality ratio,  $\chi$ , at the LHC at 14 TeV for  $M_S = 5$  and 10 TeV for the SM, ADD and ADD-MLS for  $\delta = 3(6)$  XDs [*upper(lower)*] normalised to 1 and compared to the SM expectation.

## 4.2 Total cross sections

The plots of total cross section versus  $M_S$  in Fig. 5 show a similar trend to those presented in [5]. Based on the differential distributions discussed in the previous subsections, the tracking  $M_{t\bar{t}} > M_S/2$  and  $\chi < 4$  cuts were implemented. The differential cross sections were integrated up to  $0.8M_S$  and compared to the total SM cross section integrated over the same range. In this way, the reach to set lower bounds on  $M_S$  was determined for the case of non-observation of a deviation at 95% CL for an assumed integrated luminosity of 100(5)[4]  $\text{fb}^{-1}$  at the LHC(LHC)[Tevatron] with 14(7)[2] TeV. Simply plotting the total  $t\bar{t}$  production cross section as a function of  $M_S$  provided an idea of the potential to exclude regions of

$M_S$  by comparing it to the upper and lower  $2\sigma$  bounds for the SM prediction. The region of interest is where the signal becomes indistinguishable from the SM background for the assumed integrated luminosity.

In Tab. 1 we summarise the rough bounds we obtain, after assuming a total 4(3)% reconstruction efficiency of the  $t\bar{t}$  final state at the LHC(Tevatron) [32], including all possible decay channels.

Collider	Luminosity	$M_S$ (ADD)	$M_S$ (ADD+MLS)
LHC at 14 TeV	100 fb $^{-1}$	5.4 TeV	5.1 TeV
LHC at 7 TeV	5 fb $^{-1}$	2.2 TeV	2 TeV
Tevatron at 2 TeV	4 fb $^{-1}$	<1 TeV	<0.8 TeV

Table 1: The 95% CL limits on the reach to set bounds on  $M_S$  in ADD and ADD-MLS at the three collider benchmarks considered. The efficiency of reconstructing the  $t\bar{t}$  final states in all possible decay channels is included and cuts on  $M_{t\bar{t}}$  and  $\chi$  were enforced, as described in the text.

### 4.3 Luminosity dependence

Finally, having assessed that the Tevatron scope is rather limited, we end the numerical analysis by taking some benchmark  $M_S$  values for the LHC at 7 and 14 TeV and computing the corresponding integrated cross sections in order to determine the potential significance,  $S/\sqrt{B}$ , that could be obtained at the LHC collider as a function of the integrated luminosity, where  $S$  and  $B$  represent the number of signal and background events, respectively. The aforementioned  $M_S/2 < M_{t\bar{t}} < 0.8M_S$  and  $\chi < 4$  cuts were used. The significances are shown in Fig. 6 for values of  $M_S$  that should be visible at the two LHC configurations, according to the results of subsec. 4.2. These results are consistent with those in the previous subsection for the assumed values of integrated luminosity and show in perspective that such models are further testable and clearly distinguishable from each other not only by the LHC at 14 TeV but also, to an understandably more limited extent, by the LHC at 7 TeV, with increasing data.

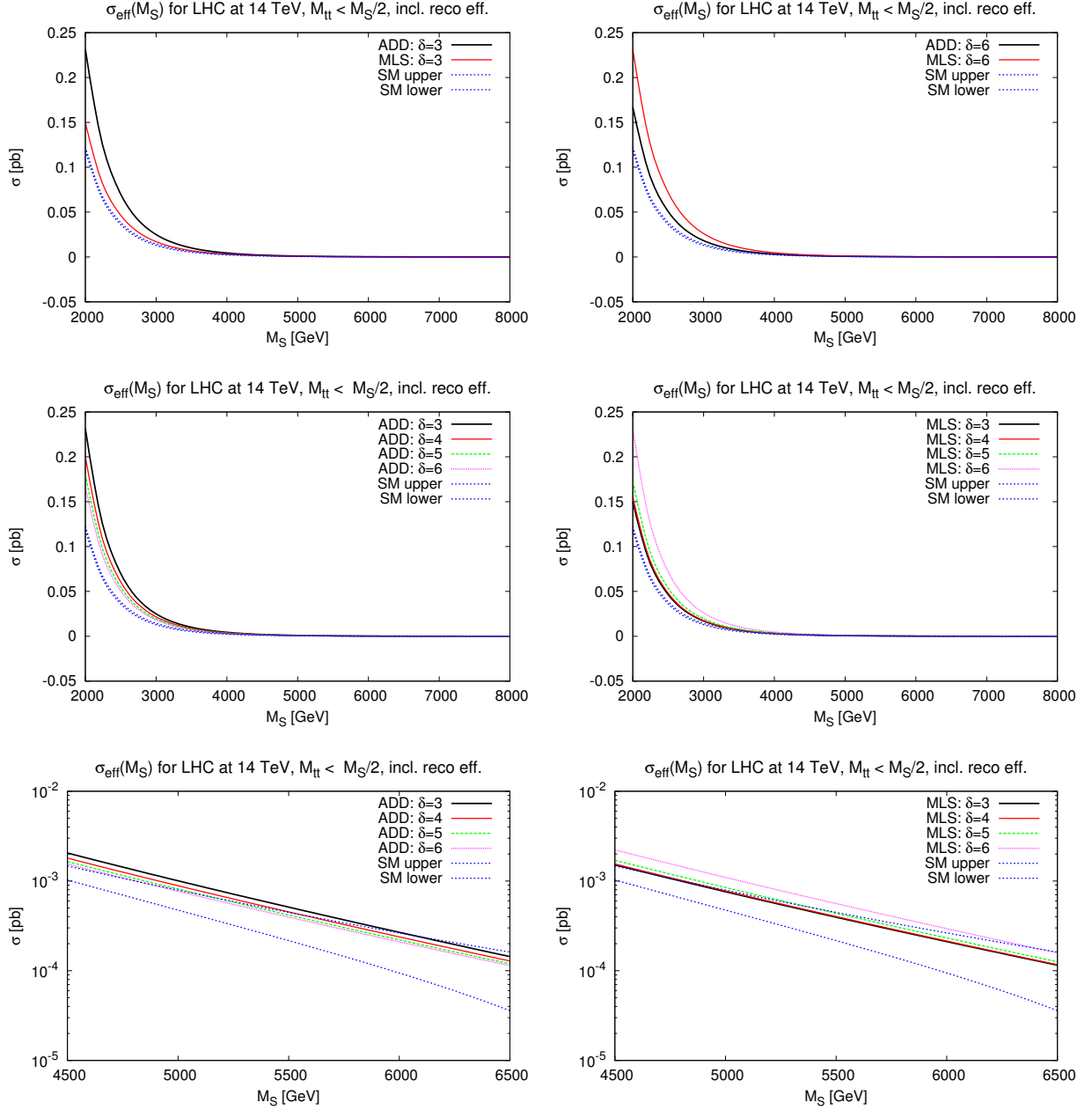


Figure 5: *Upper:* Total cross section for  $pp \rightarrow t\bar{t}$  at the LHC with  $\sqrt{s} = 14$  TeV as a function of  $M_S$  for  $\delta = 3, 6$  XDs comparing ADD and ADD-MLS.

*Middle:* Total cross section for  $pp \rightarrow t\bar{t}$  at the LHC with  $\sqrt{s} = 14$  TeV as a function of  $M_S$  for  $\delta = 3 - 6$  XDs in ADD and ADD-MLS separately.

*Lower:* Close-up on regions of interest in the above two plots. Also plotted are the SM 95% confidence level (CL) upper and lower bounds for  $100 \text{ fb}^{-1}$  of integrated luminosity. Cuts on  $M_{t\bar{t}}$  and  $\chi$  were enforced and an estimate of the  $t\bar{t}$  reconstruction efficiency folded in, as described in the text.

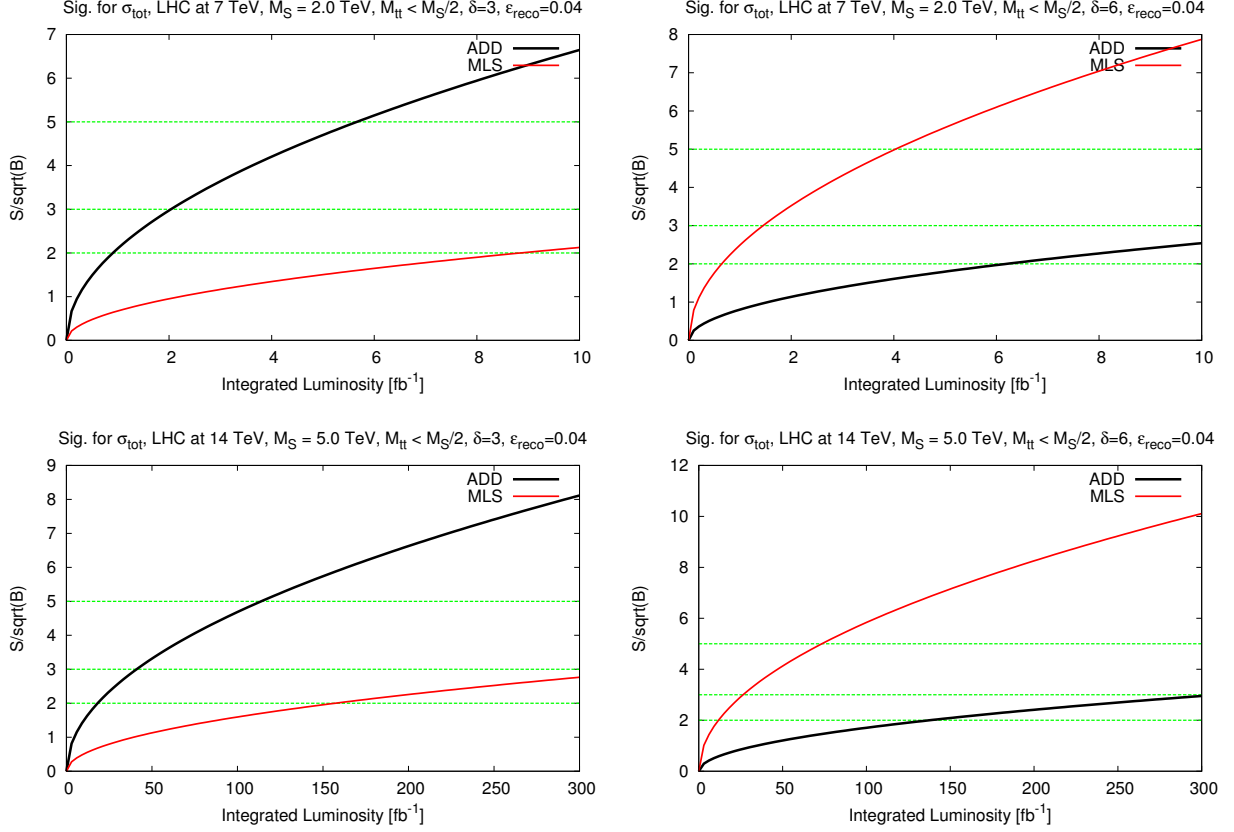


Figure 6: Significance,  $\sigma = S/\sqrt{B}$ , of the ADD and ADD-MLS with  $M_S = 2(5)$  TeV,  $\delta = 3, 6$  as a function of the integrated luminosity for the LHC at 7(14) TeV [*upper(lower)*]. This is calculated from the cross sections obtained imposing the tracking  $M_S/2 < M_{tt} < 0.8M_S$  and  $\chi < 4$  cuts. Lines of  $\sigma = 2, 3, 5$  are plotted for reference.

## 5 Conclusions

In summary, the  $t\bar{t}$  channel at the LHC shows some promise in being able to access and set bounds on the parameters of the ADD model with and without the MLS extension, specifically, when  $M_S \leq 5$  TeV for  $\delta = 3 - 6$ , assuming design energy and luminosity. Compared to a similar study conducted in the DY channel, the limited efficiency in reconstructing  $t\bar{t}$  pairs (with respect to  $e^+e^-$  and  $\mu^+\mu^-$  pairs) means that the bounds obtained in this study may not quite surpass those suggested in [5]. The early data LHC setup has a more limited but still relevant reach ( $M_S \simeq 2$  TeV for  $\delta = 3 - 6$ ) while the Tevatron always performs badly in the  $t\bar{t}$  channel, mainly due to the lower energy and dominance of the  $q\bar{q}$  initial state, which has no ADD/SM interference term. Notwithstanding, it is clear that this channel can prove useful in probing such XD models as a complement to other, perhaps ‘cleaner’ channels, such as DY, not only in measurements of the total cross section but also by considering differential distributions such as the invariant mass of the top quark pair and its centrality ratio. We have in fact shown that these distributions could reveal significant deviations from the SM predictions for values of  $M_S$  up to around 5(2.5) TeV for the LHC at 14(7) TeV and could merit further inquiry.

In the MLS extension of the ADD model, an alternative method for regulating the UV divergences of the virtual KK graviton sum has been explored. We have shown that it tames some undesirable behaviour of the ADD cross section using a natural prescription inspired by String theory considerations as one approaches the effective cutoff of such models,  $M_S$ , thereby avoiding any potential pathological overestimate of the cross sections involved. In the context of collider phenomenology, this scenario would have the effect of lowering the reach of the LHC to set bounds on or extract  $M_S$  as a consequence of its regulating properties.

Finally, it is also worth remembering here that our results are based on tree-level calculations, as NLO results in the ADD model (and modifications thereof) are not available yet. Our exercises should therefore eventually be repeated in presence of higher order effects, though we do not expect the gross features obtained here to change dramatically.

## Acknowledgments

This work is financed in part by the NExT Institute and STFC (Swindon, UK). We thank K. Sridhar and S. Biswal for their collaboration during the initial stages of this work. KM thanks the Tata Institute for Fundamental Research (Mumbai, India) and the University of Southampton (through an International Fund grant) for travel support during a visit to India, where part of the work took place.

## References

- [1] N. Arkani-Hamed, S. Dimopoulos, and G. Dvali, Physics Letters B **429**, 263 (1998).
- [2] I. Antoniadis, N. Arkani-Hamed, S. Dimopoulos, and G. Dvali, Phys. Lett. B **436:257-263** (1998), hep-ph/9804398.
- [3] E. Witten, Physics Today **49**, 24 (1996).
- [4] S. Hossenfelder *et al.*, Phys. Lett. **B575**, 85 (2003), hep-th/0305262.
- [5] G. Bhattacharyya, P. Mathews, K. Rao, and K. Sridhar, Phys. Lett. **B603**, 46 (2004), hep-ph/0408295.
- [6] M. Arai, N. Okada, K. Smolek, and V. Simak, Phys. Rev. D **70:115015,2004** (Phys.Rev.D70:115015,2004), hep-ph/0409273.
- [7] C. Csaki, (2007), hep-ph/0404096.
- [8] T. Han, J. D. Lykken, and R.-J. Zhang, Phys. Rev. **D59**, 105006 (1999), hep-ph/9811350.
- [9] G. F. Giudice, R. Rattazzi, and J. D. Wells, Nucl. Phys. **B544**, 3 (1999), hep-ph/9811291.
- [10] W. G. Unruh, Phys. Rev. D **51**, 2827 (1995).
- [11] A. Kempf, G. Mangano, and R. B. Mann, Phys. Rev. D **52**, 1108 (1995).
- [12] A. Kempf and G. Mangano, Phys. Rev. D **55**, 7909 (1997).
- [13] J. Magueijo and L. Smolin, Phys. Rev. Lett. **88**, 190403 (2002), hep-th/0112090.
- [14] J. Magueijo and L. Smolin, Phys. Rev. D **67**, 044017 (2003), gr-qc/0207085.
- [15] B. Mu, H. Wu, and H. Yang, Chin. Phys. Lett. **28**, 091101 (2011), 0909.3635.
- [16] P. Mathews, S. Raychaudhuri, and K. Sridhar, Phys. Lett. **B450**, 343 (1999), hep-ph/9811501.
- [17] T. Stelzer and W. F. Long, Comput. Phys. Commun. **81**, 357 (1994), hep-ph/9401258.
- [18] R. Franceschini, P. P. Giardino, G. F. Giudice, P. Lodone, and A. Strumia, JHEP **05**, 092 (2011), 1101.4919.
- [19] See <http://hep.pa.msu.edu/cteq/public/cteq6.html>.
- [20] P. Nason, S. Dawson, and R. K. Ellis, Nucl. Phys. **B303**, 607 (1988).

- [21] W. Beenakker, W. L. van Neerven, R. Meng, G. A. Schuler, and J. Smith, Nucl. Phys. **B351**, 507 (1991).
- [22] W. Bernreuther, A. Brandenburg, Z. Si, and P. Uwer, Nucl. Phys. **B690**, 81 (2004), hep-ph/0403035.
- [23] N. Kidonakis and R. Vogt, Phys. Rev. D **78:074005** (2008), 0805.3844.
- [24] M. Cacciari, S. Frixione, M. L. Mangano, P. Nason, and G. Ridolfi, JHEP **0809:127** (2008), 0804.2800.
- [25] M. Czakon and A. Mitov, Nucl. Phys. B **824:111-135** (2008), 0811.4119.
- [26] K. Melnikov and M. Schulze, JHEP **0908:049** (2009), 0907.3090.
- [27] A. Bredenstein, A. Denner, S. Dittmaier, and S. Pozzorini, (2010), 1001.4006.
- [28] S. Moretti, M. R. Nolten, and D. A. Ross, Phys. Lett. B **639:513-519** (2006;), hep-ph/0603083.
- [29] J. H. Kuhn, A. Scharf, and P. Uwer, Eur. Phys. J. C **51:37-53** (2007), hep-ph/0610335.
- [30] W. Hollik and M. Kollar, Phys. Rev. D **77:014008** (2007), 0708.1697.
- [31] W. Bernreuther, M. Fückler, and Z.-G. Si, Phys. Rev. D **74**, 113005 (2006).
- [32] A. de Roeck, A. Ball, M. Della Negra, L. Fo, and A. Petrilli, *CMS physics: Technical Design Report* (CERN, Geneva, 2006).
- [33] CDF IIb, P. T. Lukens, FERMILAB-TM-2198.